Cell Transplantation, Vol. 19, pp. 1659–1670, 2010
Printed in the USA.

0963-6897/10 $90.00 + .00
DOI: 10.3727/096368910X516619
E-ISSN 1555-3892
www.cognizantcommunication.com

Intravital Two-Photon Microscopy Assessment of Renal Protection Efficacy of siRNA for p53 in Experimental Rat Kidney Transplantation Models

Ryoichi Imamura,* Yoshitaka Isaka,† Ruben M. Sandoval,‡ Asaf Ori,§ Swetlana Adamsky,§ Elena Feinstein,§ Bruce A. Molitoris,‡ and Shiro Takahara¶

*Department of Urology, Osaka University Graduate School of Medicine, Osaka, Japan
†Department of Nephrology, Osaka University Graduate School of Medicine, Osaka, Japan
‡Department of Medicine, Division of Nephrology, Indiana Center for Biological Microscopy, Indiana University, Bloomington, IN, USA
§Quark Pharmaceuticals Inc., Fremont, CA, USA
¶Department of Advanced Technology for Transplantation, Osaka University Graduate School of Medicine, Osaka, Japan

Renal ischemia-reperfusion (I/R) injury, which is unavoidable in renal transplantation, frequently influences both short- and long-term allograft survival. Despite decades of laboratory and clinical investigations, and the advent of renal replacement therapy, the overall mortality rate due to acute tubular injury has changed little. I/R-induced DNA damage results in p53 activation in proximal tubule cells (PTC), leading to their apoptosis. Therefore, we examined the therapeutic effect of temporary p53 inhibition in two rat renal transplantation models on structural and functional aspects of injury using intravital two-photon microscopy. Nephrectomized Sprague-Dawley rats received syngeneic left kidney transplantation either after 40 min of intentional warm ischemia or after combined 5-h cold and 30-min warm ischemia of the graft. Intravenously administrated siRNA for p53 (siP53) has previously been shown to be filtered and reabsorbed by proximal tubular epithelial cells following the warm ischemia/reperfusion injury in a renal clamp model. Here, we showed that it was also taken up by PTC following 5 h of cold ischemia. Compared to saline-treated recipients, treatment with siP53 resulted in conservation of renal function and significantly suppressed the I/R-induced increase in serum creatinine in both kidney transplantation models. Intravital two-photon microscopy revealed that siP53 significantly ameliorated structural and functional damage to the kidney assessed by quantification of tubular cast formation and the number of apoptotic and necrotic tubular cells and by evaluation of blood flow rate. In conclusion, systemic administration of siRNA for p53 is a promising new approach to protect kidneys from I/R injury in renal transplantation.

Key words: Apoptosis; p53; Ischemia-reperfusion injury; Kidney; Small interfering RNA (siRNA)

INTRODUCTION

Clinical and experimental evidence suggest that ischemia-reperfusion (I/R) injury to kidney grafts may influence both early and late transplant function (29). Ischemia followed by reperfusion is closely related to the pathogenesis of early graft damage. Overall, ischemia in a kidney graft is the sum of possible transient warm ischemia during allograft removal from the donor and the transplantation operation, and cold ischemia associated with graft preservation and storage (28). Reperfusion, which is critical to the viability of the transplanted organ, induces additional damage (23). I/R injury is characterized histologically by inflammation and tubular cell death in the form of apoptosis and/or necrosis (10,30). Although the relative importance of these two forms of cell death in determining the functional outcome of injury remains poorly understood, we demonstrated that preventing apoptosis is protective also against other components of renal I/R injury (17,27).

We and others have documented the importance of p53 activation in I/R injury to the kidney and other organs (7–9,15,18,19). Moreover, we have demonstrated that pharmacological inhibition of p53 using either small molecule (19) or systemically delivered small interfering RNA (siRNA) targeting p53 (24) minimized acute I/R injury to the kidney in the renal clamp model.

After systemic administration, siRNA tends to show

Received December 29, 2009; final acceptance June 10, 2010. Online prepub date: August 17, 2010.
Address correspondence to Yoshitaka Isaka, M.D., Ph.D., Department of Nephrology, Osaka University Graduate School of Medicine, Suita, Osaka, 565-0871 Japan. Tel: +81-6-6879- 3857; Fax: +81-6-6879-3857; E-mail: isaka@kid.med.osaka-u.ac.jp

accumulation in both the liver and kidneys (5). We have shown extensive and predominant accumulation of siRNA with phosphodiester backbone in proximal tubule cells (PTC). The internalized siRNA had relatively short tissue half-life and showed suppression of its target, p53 (24). Other investigative teams have also shown that antisense oligonucleotides and siRNA suppress activity of the target genes expressed in proximal tubular cells. Thus, suppression of renal Fas (26), caspase 3 and 8 (33), or C5a (34) have been shown to minimize ischemic injury in the kidney.

From the first in vivo application of siRNA in an animal model (22), the pace of drug development has been more rapid when compared with antisense oligonucleotides, which have been pursued as a therapeutic tool for over 20 years. Therefore, the present studies were undertaken to assess potential utility of siP53 previously used by us for renal protection in a clamp model, in other clinically relevant models of renal I/R associated with kidney transplantation. Functional analysis demonstrated efficacy of siP53 in reducing posttransplantation increases of serum creatinine levels. In addition, for the first time, we have employed intravital two-photon microscopy to examine the effect of siRNA for p53 in situ. We observed that administrated siRNA for p53 was delivered into tubular epithelial cells by endocytosis following glomerular filtration. It minimized PTC apoptosis and tubular cast formation and preserved peritubular microvascular blood flow. These studies demonstrate applicability of two-photon microscopy for quantification of structural and functional changes associated with cellular injury in the kidneys and further emphasize potential therapeutic utility of siP53 in acute kidney injury indications.

MATERIALS AND METHODS

Animal Models

Male Sprague-Dawley (SD) rats (230–280 g; Harlan, Indianapolis, IN) were used for all studies and cared for as previously described (1). All protocols were approved by the Indiana University IACUC committee.

Kidney Autotransplantation (Warm Ischemia Model). Male SD rats were anesthetized with 50 mg/kg pentobarbital sodium (Besse Scientific, Louisville, KY) before surgery and placed on a homeothermic table to maintain core body temperature at 37°C. Anesthetized animals were subjected to a midline laparotomy. Left kidneys were harvested and placed in a dish containing 0.9% NaCl for a few minutes during which time a right nephrectomy was performed on the same animal. The left kidneys were then autotransplanted, being placed into their orthotopic position. End-to-end anastomoses of the renal artery, vein, and urether were performed using 10-0 Prolene (ETHICON, Somerville, NJ). The animals were rehydrated with 1 ml of sterile saline introduced into the abdominal cavity. The muscle layer was closed with 3-0 silk; the skin was sutured with either surgical staples or silk. Total warm ischemia time (including surgical procedures) was approximately 40 min.

Syngeneic Kidney Transplantation Model (Cold Ischemia Model). Donor male SD rats were anesthetized with 50 mg/kg pentobarbital sodium (Besse Scientific) before surgery. Anesthetized animals were subjected to a midline laparotomy. Left kidney was removed and flushed via renal artery with an ice-cold preservation HTK solution (Custodiol®; Riyadh, Saudi Arabia) and placed on ice under sterile conditions for a period of 5 h. At the end of this period, a bilateral nephrectomy was performed on a similarly anesthetized recipient rat, and the cold-preserved left kidney from a donor animal was transplanted into the recipient rat as described for kidney autotransplantation model. Additional warm ischemia period for the graft during the surgery was approximately 30 min.

Serum Creatinine Measurements

Blood samples (1 ml) were drawn from the tail vein and centrifuged. The serum was collected and stored at −20°C until the analysis. Creatinine concentrations were measured using a Creatinine Analyzer 2 (Beckman Inc.). The device was standardized with a corresponding common control, and the samples were run using a picric acid reaction.

Two-Photon Microscopy and Image Analysis

All two-photon imaging was conducted as previously optimized and described (11,25). To study triply labeled samples the fluorescence emission were split into three channels centered at 605, 525, and 455 nm, collected in separate photomultiplier tube detectors, and displayed as pure red, green, and blue, respectively. Stacks were collected by 1-μm optical steps into the tissue to a maximal depth of 100 μm. Images and data volumes were processed using Image J software (U. S. National Institutes of Health, MD, http://rsb.info.nih.gov/ij/), Metamorph Image Processing Software (Universal Imaging-Molecular Devices, PA), and Adobe Photoshop (Adobe, CA) as previously reported (2). Fluorescent siRNA uptake was performed and imaged as previously described (24). Fluorescent probes were infused via a jugular venous line or a femoral venous line. Fluorescent probes were injected in a bolus with normal saline in a total combined volume not exceeding 0.5 ml. All probes obtained from Molecular Probes (Eugene, OR). Dyes included 500,000 Da fluorescein dextran (green) for visualizing microvascular flow and organ perfusion; 10,000 Da rhodamine dextran (red) or cascade blue dextran (blue) for visualiz-

ing endocytosis by proximal tubules; Hoechst 33342 (cyan) labels all nuclei and allows for identification of apoptotic nuclei; and propidium iodide (PI, red) was used to labels only necrotic nuclei. Nuclei appear white (red plus blue) when stained with both PI and Hoechst.

Quantification of Tubular Profiles Containing Cast Material. There were 35–112 fields of view per animal captured at 20× magnification. Number of cast-positive tubular profiles were determined per field of view, summarized per animal, and averaged per field. These individual animal average values were then used to calculate average number of positive profiles per view field per group.

Quantification of Apoptotic and Necrotic Cells in Tubular Profiles. Apoptotic and necrotic nuclei were identified as previously described (20). The number of dead cells was estimated per area (view field) captured at 20× magnification. There were 37–92 areas analyzed per animal, summarized per animal and averaged per field. These individual animal average values were then used to calculate average number of dead cell per view field per group.

Renal Blood Flow. Renal blood flow was measured using a modified line scan method (25,35) based on evaluation of RBC speed rate. The evaluation was performed in 20 randomly captured cortical fields, 5 randomly captured line scans of horizontal vessels within each field, and both small and large diameter vessels within the field of view were studied. The results were summarized per animal and averaged per field.

p53 ELISA Assay

The kidney was ground to powder by mortar and pestle in liquid nitrogen. The powder was lyzed in an ice-cold lysis buffer 1 (0.1 M Tris, pH 7.5, 1 mM EDTA, 1 mM EGTA, 2 mM DTT, 20 mM NaF, 4 mM $Na_4P_2O_7$, 4 mM b-glycerophosphate, 20 mM $ZnSO_4$, 1 tablet of protease inhibitors per 20-ml solution). One gram of ground kidney tissue was mixed with 5 ml of buffer 1 and then further homogenized using Pro2000 homogenizer for 5–10 s. The homogenate was incubated for 40 min on ice while gently shaking. An equal volume of buffer 2 (20% glycerol, 800 mM NaCl) was added to the homogenate while gently vortexing. After a second cycle of incubation for 40 min on ice with gentle shaking, the lysate was subjected to ultracentrifugation at $100{,}000 \times g$ for 1 h at 40°. The cleared supernatant was aliquoted and snap-frozen in liquid nitrogen until used.

For ELISA, black clear bottom plates were coated with mouse anti-p53 MoAb DO-7 (Santa Cruz) in a carbonate buffer (100 µl/well), at a final concentration of 2 µg/ml, and incubated at 4°C overnight. The plates were washed three times with 300 µl/well PBS, and further blocked with StartingBlock solution (Pierce, 350 µl/well) at 37°C for 2 h. Then, the plates were again washed three times with 300 µl/well PBS. Kidney protein extracts (0.2 mg) diluted in 1% BSA in PBS to a final volume of 100 µl were added to the wells and incubated at 25–27°C for 2 h. Unbound proteins were removed by five repeated washings with 1× TBS containing 0.05% NP-40 (300 µl/well). Next, rabbit anti-p53 polyclonal antibodies FL-393 (Santa Cruz) were added to a final concentration of 5 µg/ml, in StartingBlock (100 µl well) and incubated for 1 h at 37°C. Unbound antibodies were removed by five consecutive washes with 1× TBS containing 0.05% NP-40 (300 µl/well). The detecting antibodies, goat-anti-rabbit $F(ab')_2$ and Fc-HRP (both from Jackson Laboratories) were diluted 1:10,000 in StartingBlock and added in a volume of 100 µl well. The plates were incubated for 1 h at 37°C. Unbound antibodies were removed by five consecutive washes of 1× TBS containing 0.05% NP-40 (300 µl/well). The reaction was developed using QuantaBlu Fluorogenic substrate kit (Pierce) according to the manufacturer's instructions.

Statistical Analysis

Statistical analysis was performed using SAS package by a qualified statistician. Values are reported as mean ± SD. Statistical significance, defined as $p < 0.01$ or $p < 0.05$, was evaluated using the Tukey test for parametric multiple comparison.

RESULTS

Efficacy of Systemic Administration of siRNA Targeting p53 in Amelioration of I/R Injury in Kidney Autotransplantation (Warm Ischemia) Model

Six to 10 SD male rats per group were subjected to kidney autotransplantation operation as described in Materials and Methods. Control animals were injected intravenously with 100 µl saline 15 min before kidney removal ($n = 10$). Experimental groups received 12 mg/kg siP53 as a 100-µl bolus intravenous injection either at 15 min before kidney removal ("15 min pre" group, $n = 6$) or at 4 h after kidney autotransplantation ("4 h post" group, $n = 6$), or both at 15 min before kidney removal and 4 h after its autotransplantation ("15 min pre + 4 h post" group, $n = 7$). siRNA dose and 4-h time point selection were based on the previous determination of the optimal conditions for siP53 efficacy in the clamp I/R acute kidney injury model (24). The animals from the latter group received a total of 24 mg/kg siP53 in two injections. Serum creatinine levels served to quantify functional efficacy end point and were measured at 24 and 48 h and at 1 week after autotransplantation. In the course of the study, kidneys of some randomly se-

lected operated animals from all groups were subjected to intravital two-photon microscopy analysis.

siP53 Treatment Attenuates Serum Creatinine Increase Following Kidney Autotransplantation

In all siP53 treatment regimens tested, serum creatinine levels were lower than those in the control group (Fig. 1). Despite of the obviously lower serum creatinine levels in all siP53-treated groups, the difference between each of the treatment groups and the control group at all time points was not significant (adjusted value $p > 0.90$) when evaluated as repeated measurements. This effect was due to a rapid normalization of serum creatinine levels in the control group at 48-h and 1-week postoperation time points. Because serum creatinine levels in this model peaked at 24 h posttransplantation, followed by a quick normalization, the statistical differences between control and siP53 treatment groups were addressed independently at the 24-h time point. As shown in Figure 1, at this time point all siRNA-treated groups had serum creatinine levels significantly lower than those in the control untreated transplant group. No significant differences in reduction of serum creatinine levels were found among the three different siRNA treatment regimes used, although the postoperation treatment seemed to be more effective than the preoperation one.

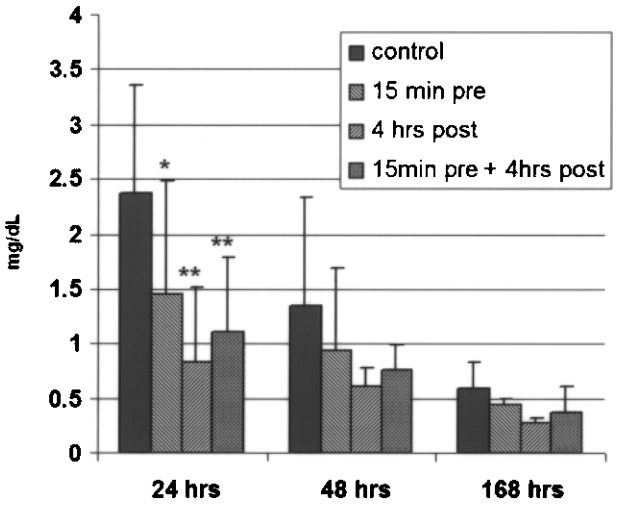

Figure 1. Changes of serum creatinine levels in rats subjected to kidney autotransplantation operation (warm ischemia). Groups of 6–10 rats were subjected to kidney autotransplantation operation (see Materials and Methods and Results for details). Serum creatinine levels were measured at 24, 48, and 168 h (1 week) after the operation. Control group was treated with equal volume of PBS. Other groups were treated with 12 mg/kg siRNA targeting p53 at the following times in regard to the operation: 15 min before kidney removal (15 min pre); 4 h after anastomosis and restoration of blood flow (4 h post); at both time points (15 min pre + 4 h post). Statistical analysis was performed using one-way ANOVA on serum creatinine values at 24 h postoperation time point. *$p < 0.05$ compared to control; **$p < 0.01$ compared to control. Data represent mean ± SD.

siP53 Treatment Reduces Cast Occurrence in the Transplanted Kidney

Intravital two-photon analysis of tubular cell injury was undertaken. As is shown in Figure 2, remarkably more 10-kDa cascade blue dextran was endocytosed by PTC in siRNA-treated rats (compare Fig. 2B vs. A). In SD rats, it is difficult to quantify PTC endocytosis as the different tubular segments cannot be identified in these outer cortical fields. However, cast formation was easily quantified and slowed markedly fewer casts in siRNA-treated rats (Fig. 2C). Because these were terminal studies, as nuclear marker dyes were used, the number of animals analyzed was limited. Comparison of control group ($n = 3$) with all siP53-treated animals as a joint group ($n = 5$) revealed statistically significant difference at 24 h after the transplantation ($p < 0.01$). At 1 week after the operation, the results for control and treated groups did not show statistical difference due to improvement in control rats.

siP53 Treatment Reduces Frequency of Apoptotic/ Necrotic Cells in the Transplanted Kidney

Intravital two-photon microscopy was also used to quantify apoptosis and necrosis in outer cortical PTC at 24 h posttransplantation. Again, administration of siRNA to p53 markedly reduced the combined number of apoptotic and necrotic cells (dead cells). All three siP53 treatment groups demonstrated a positive response and this difference was statistically different if a comparison was made between untreated ($n = 3$) and siRNA treated ($n = 5$) rats ($p < 0.01$) (Fig. 3).

siP53 Treatment Improves Blood Flow in the Transplanted Kidney

Microvascular RBC flow rates were analyzed using line scan techniques, as we have previously reported (25,35). Microvessels of different diameter within a given random field were quantified. RBC flow rates were significantly improved by treatment with siRNA 4 h posttransplant ($p < 0.01$) and by pre- and posttreatment ($p < 0.05$) at both 24 and 48 h posttransplant. This was not true for siRNA pretreatment at either 24- or 48-h time points (Fig. 4).

siP53 Treatment Reduces p53 Levels in the Transplanted Kidney

At the time of the experiment termination (1 week after the operation), the kidneys were harvested and used for analysis of p53 protein expression by a quantitative sandwich ELISA. Whereas p53 protein levels in PBS-treated operated animals were approximately fourfold

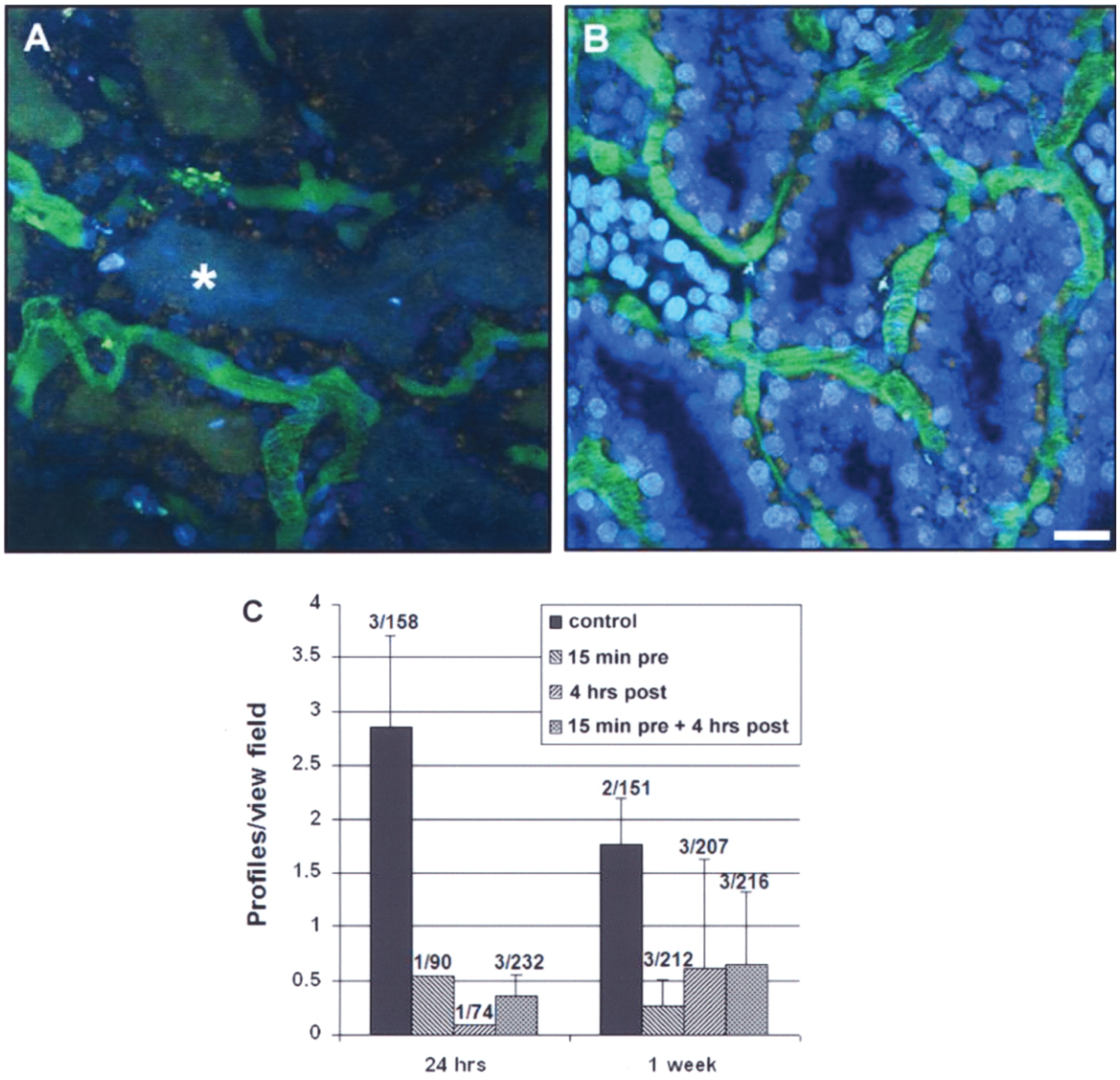

Figure 2. siRNA targeting p53 reduces tubular damage and cast formation in kidney tissue after warm I/R injury. To assess the effect of siP53 on tubular damage, intravital two-photon microscopy was used. Normal kidneys injected with 10-kDa dextran labeled with cascade blue, showed rapid accumulation in endosomes of the proximal tubules (not shown). Saline-treated transplant recipients (A) failed to take up cascade blue-labeled dextran in the proximal tubules, while siP53-treated transplant recipient rats showed preserved endocytotic function (B). In addition, cast formation (*) was diffusely observed in saline-treated rats. Quantitative analysis of cast formation, expressed as a number of tubular profile containing casts per view field at low magnification (20×), is shown in (C). Data represent mean ± SD. The numbers above the histogram bars (*x*/*y*) indicate the number of individual animals analyzed per group per time point (*x*) and total number of view fields analyzed per group (*y*). For details, see Materials and Methods. Scale bar: 20 μm (A, B).

higher than at baseline, they were only slightly elevated (~1.5-fold) in the extracts from groups treated with siP53. Because we have previously shown that RNAi in proximal tubular cells was relatively short (maximum 3 days) (24), the observed difference in p53 protein levels between saline- and siP53-treated groups at 1 week after administration rather has to be attributed to a lesser kidney injury in siP53 groups compared to control. In fact, p53 protein levels in the treated groups were still above baseline (Fig. 5).

Efficacy of Systemic Administration of siRNA Targeting p53 in Amelioration of I/R Injury in Kidney Transplantation (Cold Ischemia) Model

Because in clinical practice donor kidneys are frequently subjected not only to warm but also to cold is-

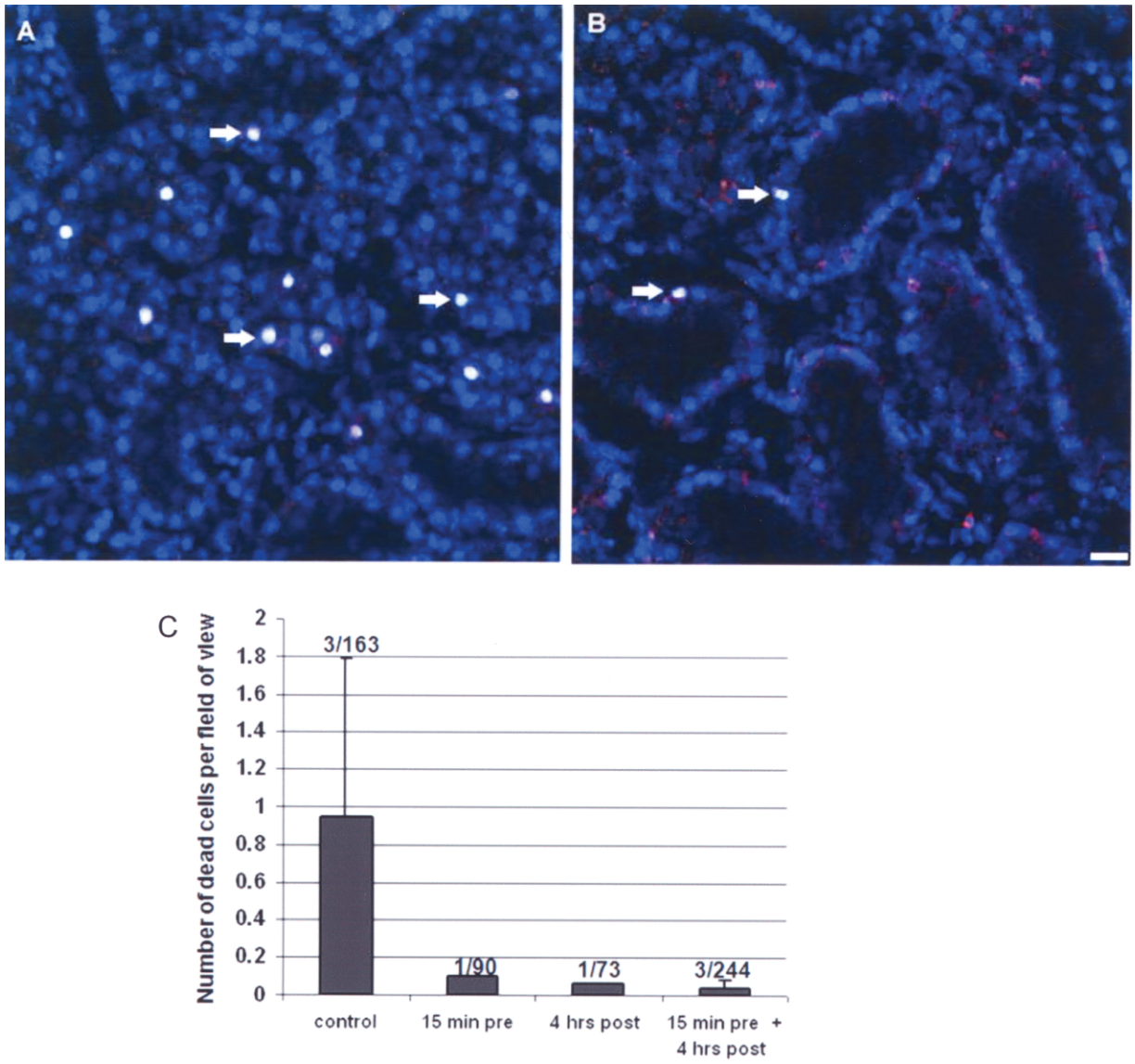

Figure 3. siRNA targeting p53 ameliorates apoptotic and necrotic injury in transplanted kidneys examined 24 h after warm I/R injury. Through the use of two nuclear dyes (cell permeant Hoechst 33342 shown in blue; and cell impermeant propidium iodide show in red) a profile of apoptosis (condensed nuclei) and necrosis (propidium iodide labeled) was generated to quantify injury. (A) Intravital two-photon images of a saline-treated transplanted kidney show numerous necrotic cells (arrows) as is evident by incorporation of the cell impermeant propidium iodide causing a white nucleus. Administration of P53 siRNA 15 min prior and/or 4 h post-kidney transplant reduced injury as seen in (B). (C) A graph displaying data from scored images shows that administration of siP53 prior to and/or postoperation reduced apoptosis and necrosis (cumulative "dead cells") associated with ischemic injury. Data represent mean ± SD. The numbers above the histogram bars (*x*/*y*) indicate the number of individual animals analyzed per group per time point (*x*) and total number of view fields analyzed per group (*y*). For details, see Materials and Methods. Scale bar: 20 μm (A, B).

chemia prior to transplantation, we next studied the effect of systemic administration of siRNA targeting p53 in a cold ischemia model of kidney transplantation in rats. Initial studies were conducted to document PTC uptake of siRNA with the previously described technique using Cy3-labeled siRNA (24). In Figure 6A, a single confocal plane is shown, and in Figure 6B a reconstructed image comprising 10 planes is shown. Proximal tubule cells in each PT rapidly took up the red fluorescent siRNA, but at variable levels.

Figure 6C shows the serum creatinine results at 24, 48, and 168 h posttransplantation. Male SD rats (5–6 per group) were subjected to cold ischemia kidney transplantation operation as described in Materials and Meth-

ods. Control transplant recipients ($n = 6$) were injected intravenously with 100 µl saline 15 min after the restoration of blood flow in the graft. Experimental groups received 12 mg/kg siP53 as 100-µl bolus intravenous injection either to donors given at 30 min before kidney removal ("Donor 30 min" group; $n = 6$) or to recipients at 15 min or at 4 h after the transplantation ["Recipient 15 min" ($n = 5$) and "Recipient 4 h" ($n = 6$) groups, respectively]. Serum creatinine levels served as the functional efficacy end point and were measured at 24 and 48 h and at 1 week after the operation. The data analysis demonstrated that siP53 treatment given either to donors prior to kidney harvesting or to transplant recipients at either time point significantly reduced serum creatinine levels as early as 24 h posttransplantation compared to the control group (Fig. 6C). Although no significant dif-

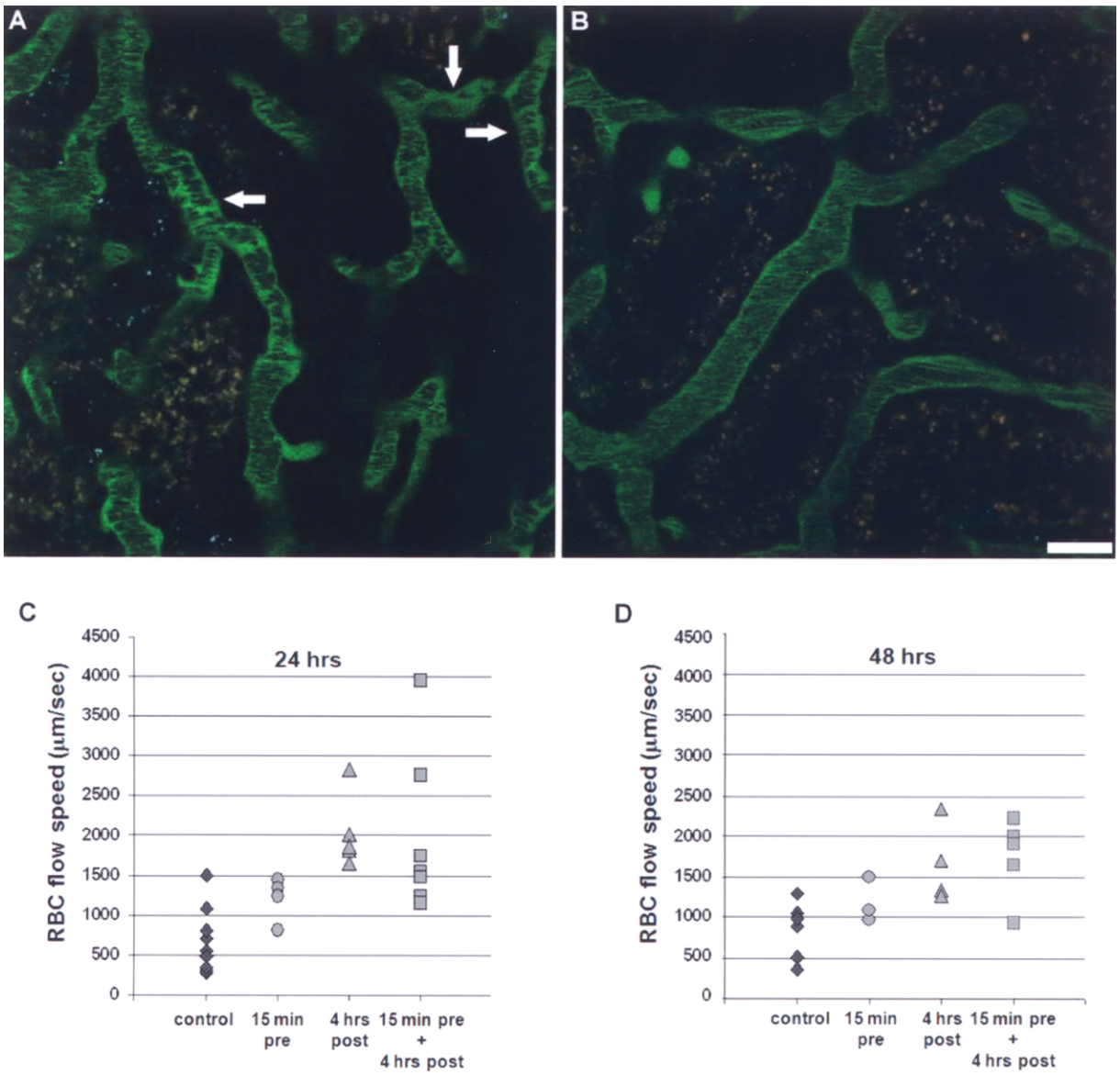

Figure 4. p53 siRNA improved blood flow in kidneys following warm renal I/R injury. (A) Saline-treated warm kidney transplant ischemia rats imaged 24 h after injury exhibited a reduction in the speed of red blood cells quantified by linescan technique. Note the sluggish flow and increased area occupied by plasma in many of the small vessels (arrows). In contrast, p53 siRNA-treated transplanted kidney rats exhibited fewer disruptions in RBC flow 24 h after renal injury panel (B). (C, D) Quantitative differences in RBC flow in P53 siRNA-treated and untreated rats at both 24 and 48 h after the operation, respectively. Individual data are shown. Quantitation was done on images acquired using a linescan technique to maximize temporal resolution. See Materials and Methods for details. Scale bar: 20 µm (A, B).

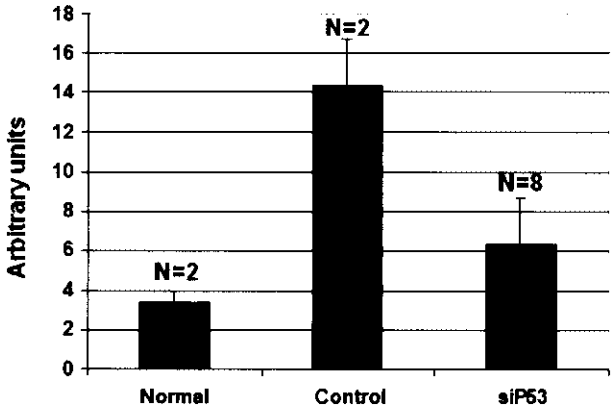

Figure 5. Measurement of p53 protein levels in the injured kidneys 1 week after the autotransplantation operation. p53 protein levels were assessed in kidney lysates using sandwich ELISA. All ELISA reactions were performed twice on each protein extract. siP53 group contains animals treated with siRNA in all three regiments (pretreatment, posttreatment, and combination of both). Differences among all groups are statistically significant ($p < 0.01$). Data represent mean ± SD.

ferences were detected among all siP53 treatment groups, it seems that siRNA administration to graft recipients shortly after the transplantation was more effective compared to donor treatment or to a delayed (at 4 h after transplantation) recipient treatment. In contrast to the autotransplantation warm ischemia model, exposure of kidney grafts to cold ischemia prior to transplantation resulted in elevated (1.25 mg/dl) serum creatinine levels in the control group even at 1 week posttransplantation, indicating delayed graft function (Figs. 6C and 7). At the same time, siP53-treated animals displayed a sharper decline of serum creatinine that was almost twofold lower (around 0.6 mg/dl) than in untreated control rats at 1 week posttransplantation. This decrease occurred more quickly in siP53-treated recipients compared to the group in which donors received siP53 treatment. In the former groups serum creatinine was decreased to 0.7 mg/dl already at 2 days after kidney transplantation.

DISCUSSION

The results of these studies add additional support to the therapeutic potential of the temporary inhibition of p53 expression to protect proximal tubule cells from acute injury, and further demonstrate that synthetic siRNAs represent an effective means for eliciting such activity in the kidney following intravenous administration. For these studies we utilized doses and timing strategies previously developed in a clamp model of ischemia (24). Effective therapeutic use of siRNA depends on the ability to specifically suppress expression of target proteins, in target cells, contributing to the progression of injury or disease in target cells. We show here that the kidney, and in particular the proximal tubule epithelium, is a uniquely favorable target for synthetic siRNA accumulation and action following intravenous administration even after combined cold and warm ischemia of kidney graft. Effective siRNA delivery and therapeutic efficacy were achieved without the need for either local delivery into renal vessels, or systemic hydrodynamic administration as attempted before (16) or complicated formulation with delivery-enhancing agents.

In our previous study the use of two-photon fluorescence kidney imaging, with confirmation by in situ siRNA detection using hybridization, provided insight into the spatial and temporal distribution of the siRNA. This technique affords the spatial resolution to precisely localize the siRNA to specific cell types, and the distribution of labeled siRNA in the kidney could be followed in the same animal over a time scale, giving information about the rate of metabolism of the siRNA. In the present study we utilized intravital two-photon microscopy to evaluate and quantify tubular and microvasular injury as mechanisms of the reduced functional capacity of the kidney. Inhibition of p53 by siRNA resulted in fewer apoptotic and necrotic cells, tubular casts, increased PTC endocytosis, and improved RBC flow rates. The present study also documented effectiveness of siRNA delivery and function following combined cold/warm ischemia and reperfusion injury (Fig. 6).

The results of the present study prove that p53 is an ideal therapeutic target in renal transplantation with I/R injury. I/R-induced tissue injury causes significant morbidity and mortality in patients with renal disease. Tubular epithelial and endothelial cell death may contribute to the hypoxic, as well as the reperfusion, components of this injury. These findings are in line with various in vivo and in vitro reports showing that renal apoptosis after ischemia is induced by hypoxia (3) and ATP depletion (21). Furthermore, several studies suggest that upregulated p53, a transcription factor established for apoptosis, senescence, and repair in response to a variety of cellular stress (12,31), is associated with I/R-induced cell death (19,32). DNA damage is sensed by the ataxia telangiectasia mutated (ATM) and ATM and Rad3-related (ATR) kinases. The signal is transmitted via phosphorylation of CHEK2 (CHK2 checkpoint homolog) and p53. CHEK2 also directly phosphorylates p53. Activated p53 induces the transcription of genes responsible for cell cycle arrest and DNA repair. In the case of extensive DNA damage, apoptotic pathways are induced (6). Therefore, temporary inhibition of p53 by siRNA may be reasonable to protect kidneys from acute kidney injury in transplantation.

Oligonucleotides used in this present study were modified by 2′-*O*-methylation (24), which effectively

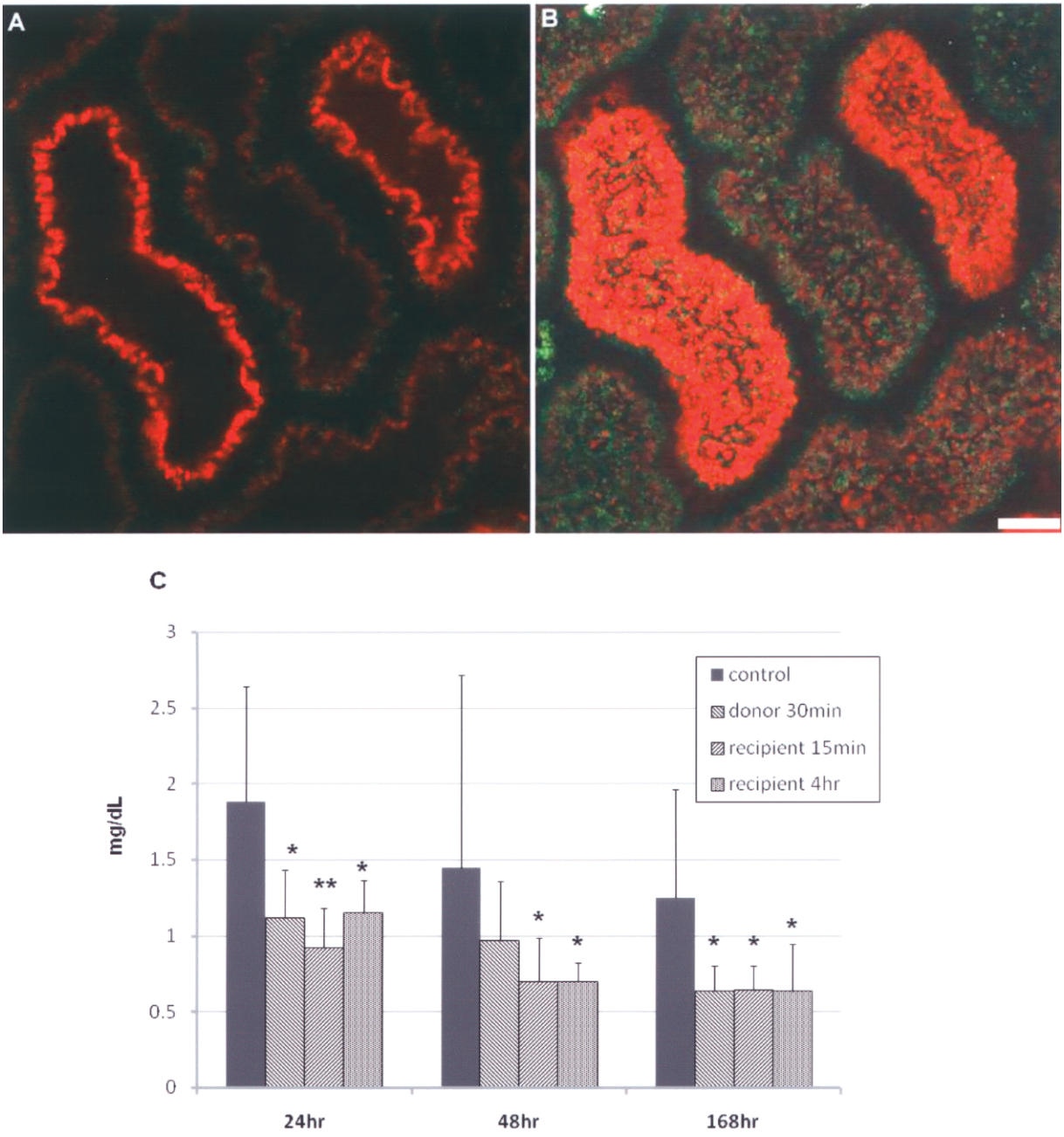

Figure 6. Assessment of kidney function following cold ischemia transplantation model. (A, B) Cy3-labeled siRNA glomerular filtration and uptake by proximal tubules. (A) A 1-µm-thick plane intravital two-photon image collected in a transplanted kidney 24 h after transplantation. Note the binding and uptake that occurs at the apical region of PTC approximately 9 min after a single IV bolus infusion of labeled siRNA. (B) A 3D reconstruction of a 10-µm thickness in the same image field. (C) Serum creatinine levels in different treatment groups at 24, 48, and 168 h after the operation. For experimental details and statistical analysis, see Materials and Methods and Results sections. *$p < 0.05$ compared to control; **$p < 0.01$ compared to control. Data represent mean ± SD. Scale bar: 20µm (A, B).

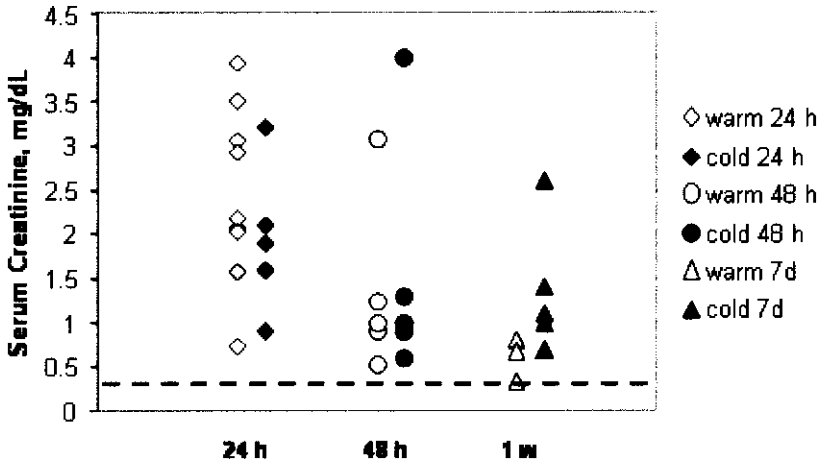

Figure 7. Time-dependent changes in serum creatinine levels in warm and in cold ischemia rat kidney transplantation models. Serum creatinine levels were measured in control animals at 24 and 48 h and at 1 week posttransplantation. Red symbols represent serum creatinine levels of individual control animals from warm ischemia/autotransplantation model; blue symbols are from combined warm and cold ischemia/transplantation model. Dashed black line in the bottom of the graph indicates normal basal serum creatinine levels.

stabilized them against plasma endonucleases (13), while preserving their ability to trigger the RNAi silencing machinery. Oligonucleotides with this stabilizing modification have a relatively low affinity for albumin and other plasma proteins (14), thus diminishing their distribution to the liver and facilitating renal clearance/uptake.

Two models of rat renal transplantation were utilized in this study. Warm ischemia/reperfusion alone or in combination with a cold ischemia results in kidney damage that peaks at 24 h (Fig. 7, red and blue diamonds). This similarity in kidney response continues till 48 h posttransplantation (Fig. 7, red and blue circles). However, at 1 week after the transplantation, there emerges a difference between the two models. Whereas kidney dysfunction caused by only warm ischemia/reperfusion disappeared by 1 week after the transplantation, addition of a cold ischemia period to the treatment scheme resulted in a delayed graft function (DGF) as shown by serum creatinine levels remaining on average 1.25 mg/dl compared to 0.6 mg/dl in only warm ischemia/reperfusion model (Fig. 7, blue and red triangles, respectively). According to a newly proposed definition of DGF, it was described as an absence of spontaneous decrease in serum creatinine of more than 10% per day for at least 3 consecutive days within the first week after transplantation (4). Note that in control posttransplantion rats in the warm ischemia model, the initial serum creatinine increase at 24 h had decreased by 75% by the end of the first week, almost returning to the basal levels (Figs. 1 and 7). On the contrary, in the cold ischemia model, the increase at 24 h posttransplantation of serum creatinine had only decreased by 34% at 1 week posttransplantation (Fig. 7), clearly indicating the relevance of the cold ischemia model to delayed kidney graft function. Thus, the combination of these two models allowed for the demonstration of the efficacy of siP53 treatment in both preventing acute kidney failure and protecting kidneys from the delayed graft function.

Several aspects of the data presented here enhance and expand the potential clinical application of siRNA for kidney transplantation indication. First, the kidney, and in particular the PTC, are overwhelmingly the primary site of tissue distribution following intravenous injection even in the transplanted organ. Second, the rapid clearance from the body minimizes exposure of other organs/cells. Third, the optimum administration time of siRNA (at least the one that targets p53) was found to be after the transplantation. This significantly simplifies the use of the drug in clinical trials and in practice because only the transplant recipient would be treated and, hence, only his/her consent is required.

Altogether, the above observations indicate that synthetic siRNAs represent a very favorable strategy to achieve short-term inhibition of p53 expression in PTC to protect against ischemic injury that occurs during either warm or cold ischemia preceding kidney transplantation. These results, however, offer further insight into the utilization of siRNA for modulating proximal tubular cell events with particular emphasis on the inhibition of upregulation and amplification of potentially harmful intracellular pathways.

ACKNOWLEDGMENTS: We thank Silvia Campos from the Indiana University and Esty Mishori from Quark Pharmaceuticals for her help and support of these studies. This work was funded by the grants from Quark Pharmaceuticals Inc to R.I. and B.A.M.

REFERENCES

1. Ashworth, S. L.; Sandoval, R. M.; Hosford, M.; Bamburg, J. R.; Molitoris, B. A. Ischemic injury induces ADF relocalization to the apical domain of rat proximal tubule cells. Am. J. Physiol. Renal Physiol. 280(5):F886–894; 2001.
2. Ashworth, S. L.; Sandoval, R. M.; Tanner, G. A.; Molitoris, B. A. Two-photon microscopy: Visualization of kidney dynamics. Kidney Int. 72(4):416–421; 2007.
3. Beeri, R.; Symon, Z.; Brezis, M.; Ben-Sasson, S. A.; Baehr, P. H.; Rosen, S.; Zager, R. A. Rapid DNA fragmentation from hypoxia along the thick ascending limb of rat kidneys. Kidney Int. 47(6):1806–1810; 1995.
4. Boom, H.; Paul, L. C.; de Fijter, J. W. Delayed graft function in renal transplantation. Transplant. Rev. 18(3):139–152; 2004.
5. Braasch, D. A.; Paroo, Z.; Constantinescu, A.; Ren, G.; Oz, O. K.; Mason, R. P.; Corey, D. R. Biodistribution of phosphodiester and phosphorothioate siRNA. Bioorg. Med. Chem. Lett. 14(5):1139–1143; 2004.
6. Brody, L. C. CHEKs and balances: Accounting for breast cancer. Nat. Genet. 31(1):3–4; 2002.
7. Cunningham, P. N.; Dyanov, H. M.; Park, P.; Wang, J.; Newell, K. A.; Quigg, R. J. Acute renal failure in endotoxemia is caused by TNF acting directly on TNF receptor-1 in kidney. J. Immunol. 168(11):5817–5823; 2002.
8. Daemen, M. A.; van 't Veer, C.; Denecker, G.; Heemskerk, V. H.; Wolfs, T. G.; Clauss, M.; Vandenabeele, P.; Buurman, W. A. Inhibition of apoptosis induced by ischemia-reperfusion prevents inflammation. J. Clin. Invest. 104(5):541–549; 1999.
9. Dagher, P. C. Modeling ischemia in vitro: Selective depletion of adenine and guanine nucleotide pools. Am. J. Physiol. 279(4):C1270–1277; 2000.
10. De Broe, M. E. Apoptosis in acute renal failure. Nephrol. Dial. Transplant. 16(Suppl. 6):23–26; 2001.
11. Dunn, K. W.; Sandoval, R. M.; Kelly, K. J.; Dagher, P. C.; Tanner, G. A.; Atkinson, S. J.; Bacallao, R. L.; Molitoris, B. A. Functional studies of the kidney of living animals using multicolor two-photon microscopy. Am. J. Physiol. 283(3):C905–916; 2002.
12. Fridman, J. S.; Lowe, S. W. Control of apoptosis by p53. Oncogene 22(56):9030–9040; 2003.
13. Geary, R. S.; Leeds, J. M.; Fitchett, J.; Burckin, T.; Truong, L.; Spainhour, C.; Creek, M.; Levin, A. A. Pharmacokinetics and metabolism in mice of a phosphorothioate oligonucleotide antisense inhibitor of C-raf-1 kinase expression. Drug Metab. Dispos. 25(11):1272–1281; 1997.
14. Geary, R. S.; Watanabe, T. A.; Truong, L.; Freier, S.; Lesnik, E. A.; Sioufi, N. B.; Sasmor, H.; Manoharan, M.; Levin, A. A. Pharmacokinetic properties of 2′-O-(2-methoxyethyl)-modified oligonucleotide analogs in rats. J. Pharmacol. Exp. Ther. 296(3):890–897; 2001.
15. Halterman, M. W.; Federoff, H. J. HIF-1alpha and p53 promote hypoxia-induced delayed neuronal death in models of CNS ischemia. Exp. Neurol. 159(1):65–72; 1999.
16. Hamar, P.; Song, E.; Kokeny, G.; Chen, A.; Ouyang, N.; Lieberman, J. Small interfering RNA targeting Fas protects mice against renal ischemia-reperfusion injury. Proc. Natl. Acad. Sci. USA 101(41):14883–14888; 2004.
17. Imamura, R.; Isaka, Y.; Ichimaru, N.; Takahara, S.; Okuyama, A. Carbamylated erythropoietin protects the kidneys from ischemia-reperfusion injury without stimulating erythropoiesis. Biochem. Biophys. Res. Commun. 353(3):786–792; 2007.
18. Kelly, K. J.; Plotkin, Z.; Dagher, P. C. Guanosine supplementation reduces apoptosis and protects renal function in the setting of ischemic injury. J. Clin. Invest. 108(9):1291–1298; 2001.
19. Kelly, K. J.; Plotkin, Z.; Vulgamott, S. L.; Dagher, P. C. P53 mediates the apoptotic response to GTP depletion after renal ischemia-reperfusion: Protective role of a p53 inhibitor. J. Am. Soc. Nephrol. 14(1):128–138; 2003.
20. Kelly, K. J.; Sutton, T. A.; Weathered, N.; Ray, N.; Caldwell, E. J.; Plotkin, Z.; Dagher, P. C. Minocycline inhibits apoptosis and inflammation in a rat model of ischemic renal injury. Am. J. Physiol. 287(4):F760–766; 2004.
21. Lieberthal, W.; Menza, S. A.; Levine, J. S. Graded ATP depletion can cause necrosis or apoptosis of cultured mouse proximal tubular cells. Am. J. Physiol. 274(2 Pt. 2):F315–327; 1998.
22. McCaffrey, A. P.; Meuse, L.; Pham, T. T.; Conklin, D. S.; Hannon, G. J.; Kay, M. A. RNA interference in adult mice. Nature 418(6893):38–39; 2002.
23. Menger, M. D.; Pelikan, S.; Steiner, D.; Messmer, K. Microvascular ischemia-reperfusion injury in striated muscle: Significance of "reflow paradox." Am. J. Physiol. 263(6 Pt. 2):H1901–1906; 1992.
24. Molitoris, B. A.; Dagher, P. C.; Sandoval, R. M.; Campos, S. B.; Ashush, H.; Fridman, E.; Brafman, A.; Faerman, A.; Atkinson, S. J.; Thompson, J. D.; Kalinski, H.; Skaliter, R.; Erlich, S.; Feinstein, E. siRNA targeted to p53 attenuates ischemic and cisplatin-induced acute kidney injury. J. Am. Soc. Nephrol. 20(8):1754–1764; 2009.
25. Molitoris, B. A.; Sandoval, R. M. Intravital multiphoton microscopy of dynamic renal processes. Am. J. Physiol. 288(6):F1084–1089; 2005.
26. Song, E.; Lee, S. K.; Wang, J.; Ince, N.; Ouyang, N.; Min, J.; Chen, J.; Shankar, P.; Lieberman, J. RNA interference targeting Fas protects mice from fulminant hepatitis. Nat. Med. 9(3):347–351; 2003.
27. Suzuki, C.; Isaka, Y.; Shimizu, S.; Tsujimoto, Y.; Takabatake, Y.; Ito, T.; Takahara, S.; Imai, E. Bcl-2 protects tubular epithelial cells from ischemia reperfusion injury by inhibiting apoptosis. Cell Transplant. 17(1–2):223–229; 2008.
28. Tilney, N. L.; Guttmann, R. D. Effects of initial ischemia/reperfusion injury on the transplanted kidney. Transplantation 64(7):945–947; 1997.
29. Tullius, S. G.; Tilney, N. L. Both alloantigen-dependent and -independent factors influence chronic allograft rejection. Transplantation 59(3):313–318; 1995.
30. Ueda, N.; Shah, S. V. Tubular cell damage in acute renal failure-apoptosis, necrosis, or both. Nephrol. Dial. Transplant. 15(3):318–323; 2000.
31. Vogelstein, B.; Lane, D.; Levine, A. J. Surfing the p53 network. Nature 408(6810):307–310; 2000.
32. Yoshida, T.; Sugiura, H.; Mitobe, M.; Tsuchiya, K.; Shirota, S.; Nishimura, S.; Shiohira, S.; Ito, H.; Nobori, K.; Gullans, S. R.; Akiba, T.; Nitta, K. ATF3 protects against

renal ischemia-reperfusion injury. J. Am. Soc. Nephrol. 19(2):217–224; 2008.
33. Zhang, X.; Zheng, X.; Sun, H.; Feng, B.; Chen, G.; Vladau, C.; Li, M.; Chen, D.; Suzuki, M.; Min, L.; Liu, W.; Garcia, B.; Zhong, R.; Min, W. P. Prevention of renal ischemic injury by silencing the expression of renal caspase 3 and caspase 8. Transplantation 82(12):1728–1732; 2006.
34. Zheng, X.; Zhang, X.; Feng, B.; Sun, H.; Suzuki, M.; Ichim, T.; Kubo, N.; Wong, A.; Min, L. R.; Budohn, M. E.; Garcia, B.; Jevnikar, A. H.; Min, W. P. Gene silencing of complement C5a receptor using siRNA for preventing ischemia/reperfusion injury. Am. J. Pathol. 173: 973–980; 2008.
35. Zipfel, W. R.; Williams, R. M.; Webb, W. W. Nonlinear magic: Multiphoton microscopy in the biosciences. Nat. Biotechnol. 21(11):1369–1377; 2003.